Suan Sunandha Science and Technology Journal
©2026 Faculty of Science and Technology, Suan Sunandha Rajabhat University

Comparative Study on the Optical Properties of Sm^{3+} Doped Glasses with Shell-Based and Commercial Calcium Oxide Modifiers

Natthakridta Chanthima[1, 2*], Nakarin Singkiburin[1, 2], Anon Angnanon[3, 4], Nuchjaree Kiwsakunkran[1, 2*]

[1] Physics Program, Faculty of Science and Technology, Nakhon Pathom Rajabhat University, Nakhon Pathom 73000, Thailand
[2] Center of Excellence in Glass Technology and Materials science (CEGM), Nakhon Pathom Rajabhat University, Nakhon Pathom 73000, Thailand
[3] Center of Radiation Research and Medical Imaging, Department of Radiologic Technology, Faculty of Associated Medical Sciences, Chiang Mai University, Chiang Mai 50200, Thailand
[4] Office of Research Administration, Chiang Mai University, Chiang Mai 50200, Thailand
***Corresponding author e-mail: nuchjaree.kiw@hotmail.com**

Received: *3 December 2025* / **Revised:** *1 January 2026* / **Accepted:** *22 February 2026*

Abstract

This study focuses on the optical and basic physical properties of samarium (Sm^{3+})-doped glasses prepared using calcium oxide (CaO) derived from mussel and cockle shells as glass network modifiers, and compares them with commercial CaO. X-ray fluorescence (XRF) analysis showed that the shell-derived CaO possessed high purity, with CaO content exceeding 99% after calcination at 900°C for 5 hours. X-ray diffraction (XRD) results revealed that prior to calcination, the primary phase in the shells was calcium carbonate ($CaCO_3$), while after heat treatment, the dominant phase transformed into calcium oxide (CaO). This indicates successful thermal decomposition of $CaCO_3$ and effective phase transition under the given conditions. In terms of optical properties, the shell-derived glass samples exhibited higher emission intensity and longer lifetimes compared to the commercial CaO sample. The density, refractive index, and molar volume values were comparable across all samples, suggesting that the use of shell-derived CaO does not significantly alter the physical properties of the glass. These results demonstrate the potential of shell-derived CaO as a sustainable alternative raw material for the production of luminescent glasses, contributing to environmentally friendly and cost-effective materials development.

Keywords: Glass, Samarium, Shell-derived calcium oxide, Optical properties

1. Introduction

The development and design of optical materials are of great importance in the era where optoelectronics and photonics technologies play a significant role in everyday life. These materials are especially critical in industries related to lasers, lighting, optical sensors, photonic circuits, and luminescent materials, which require excellent optical properties and tunable characteristics. Among these materials, glass is widely used due to its transparency, chemical stability, and the flexibility to tailor its composition to incorporate active dopants such as rare-earth ions (Selvi et al., 2015). Calcium oxide (CaO) is one of the key components employed in glass systems as a network modifier, significantly affecting the density, structure, and optical behavior of the glass (Kumar et al., 2019). In conventional glass manufacturing, CaO is typically sourced from commercial-grade materials, which are synthesized or processed from natural minerals such as limestone or dolomite. These processes are energy-intensive and costly, particularly when high purity and stability are required for optoelectronic applications (Beall, 1992). Alternatively, waste materials from the seafood industry, such as mussel shells and cockle shells, are commonly found in tropical countries including Thailand and contain over 95% by weight of calcium carbonate ($CaCO_3$). When calcined at high temperatures, these shells can serve as an alternative source of CaO (Bamigboye et al., 2021; Mignardi et al., 2024). Utilizing biowaste materials such as seashells to produce CaO not only reduces production costs and environmental waste but also aligns with the principles of the circular economy and sustainable development (Ellen MacArthur Foundation, 2013). The optical properties of rare-earth-

doped glasses, particularly those doped with samarium ions (Sm^{3+}), have attracted considerable interest for applications in luminescent materials and low-power lasers. Sm^{3+} ions exhibit visible light emission, particularly narrow-band orange-red emission, due to intra-4f transitions, which are of great interest for LEDs, biomedical lasers, and display devices (Ataullah et al., 2021; Elkhoshkhany et al., 2021). The optical performance of Sm^{3+} doped glass depends strongly on the host structure, including ion distribution within the glass matrix, glass composition, and the type of network modifier such as CaO. These factors influence various optical parameters, including transition intensities, absorption, emission intensity, lifetime, and CIE chromaticity coordinates (Isac et al., 2025). Based on the above considerations, this study aims to investigate and compare the optical properties of Sm^{3+} doped glasses prepared using CaO derived from different sources: commercial CaO, CaO synthesized from mussel shells, and CaO synthesized from cockle shells. The goal is to assess the potential of biogenic CaO as a sustainable and cost-effective substitute for commercial CaO. The study focuses on key optical characteristics such as absorption spectra, emission spectra, luminescence lifetime, refractive index, density, molar volume, and CIE 1931 color coordinates. The findings will provide insights into the feasibility and potential of using biowaste-derived materials in optical materials science, contributing to cost reduction, environmental friendliness, and sustainable material production in the future.

2. Materials and Methods

2.1 Sample preparation

In the preliminary phase of this study, two types of shell samples were selected: mussel shells and cockle shells. The shells of both types were obtained from the Gulf of Thailand and initially cleaned to remove contaminants and natural impurities adhering to the shell surfaces, as shown in Figure 1. After the cleaning process, all shell samples were subjected to calcination in a muffle furnace at 900°C for 5 hours to convert the material into a form suitable for subsequent analysis and experimentation. Following calcination, noticeable physical changes were observed, particularly in the shell coloration, which changed from its natural hue to white, indicating significant alterations in the internal composition of the material under high-temperature conditions as shown in Figure 2.

Figure 1. Mussel and cockle shell samples used in this study.

Figure 2. Mussel and cockle shell samples after calcination at 900°C for 5 hours.

2.2 Elemental composition and X-ray diffraction analysis of shell samples

After the calcined shell samples were allowed to cool to room temperature, they were finely ground using an appropriate milling device to obtain powder samples with sufficiently small particle size for analysis. The resulting powders were then subjected to elemental analysis using an X-ray fluorescence spectrometer (XRF) to determine the concentrations of the major chemical elements present in the shell samples. To investigate the crystalline structure of the calcined and ground shell samples, X-ray diffraction (XRD) analysis was performed using an X-ray diffractometer (XRD) equipped with a copper (Cu) X-ray source. This technique was used to identify the crystalline phases present in the samples and to compare the structural characteristics before and after calcination with high accuracy.

2.3 Preparation of glass samples using calcium oxide (CaO) derived from mussel and cockle shells as network modifiers

Glass samples were prepared using the molar composition $15CaO + 20ZnO + 1ZrO_2 + 63P_2O_5 + 1Sm_2O_3$ where CaO was sourced from either mussel shells or cockle shells, in order to compare their performance with that of commercial-grade CaO. A total of 15 grams of the mixed chemical components were thoroughly blended and placed into a crucible. The mixture was then melted at 1200°C for 3 hours. After melting, the glass melt was poured onto a graphite mold to form glass samples. The samples were subsequently annealed at 500°C for 3 hours, followed by furnace cooling to room temperature. Once cooled, the glass samples were cut and polished to a size of 1.0 × 1.5 × 0.3 cm^3, making them suitable for scientific measurements and characterization.

2.4 Measurements and optical characterization

In this study, the density of the prepared glass samples was measured using a density measurement device (Model ANDHR-200, Diethelm Company). The density was calculated according to Equation (1):

$$\rho = \frac{w_a}{w_a - w_w} \times \rho_w \qquad (g/cm^3) \qquad (1)$$

where w_a and w_w re the weights of the glass sample measured in air and water (in grams), respectively. ρ is the density of the glass sample and ρ_w is the density of water, taken as 1 g/cm^3. Based on the measured density, the molar volume of the glass sample was then calculated using Equation (2):

$$V_m = \frac{M_T}{\rho} \qquad (cm^3/mol) \qquad (2)$$

where M_T is the molar mass of the glass composition, and V_m is the molar volume.

The refractive index of the prepared glass samples was measured using an Abbe-type refractometer, specifically the Multi-Wavelength Abbe Refractometer DR-M2/M4 by ATAGO Co., Ltd. A sodium lamp emitting light at a wavelength of 589.3 nm was used as the light source. For measurement, the glass sample was placed on the refractometer prism, and the refractive index was recorded according to the instrument's operating manual. The obtained refractive index values were analyzed to evaluate the optical quality of the glass materials. To study the optical absorption properties, UV-Vis-NIR spectrophotometry was performed using a Shimadzu UV-3600 spectrophotometer at room temperature. The absorption spectra of all three glass samples were measured in the wavelength range of 200–500 nm, with a spectral resolution of 1 nm. This analysis aimed to identify absorption bands and estimate the transition intensities associated with the electronic transitions of the doped ions within the glass matrix. Photoluminescence (PL) studies were carried out using a Cary Eclipse fluorescence spectrophotometer (Agilent Technologies). Both excitation and emission spectra were measured over a wavelength range of 200–750 nm with a spectral resolution of approximately 1 nm. Additionally, luminescence decay time measurements were conducted by exciting the samples at 401 nm and recording emission at 597 nm. To evaluate the color characteristics of the emitted light, chromaticity coordinates were calculated and plotted

using the CIE 1931 chromaticity diagram (Commission Internationale de l'Éclairage). This analysis provides insight into the emission color of the Sm^{3+} doped glass samples.

3. Results and Discussion

3.1 Elemental composition and XRF analysis of shell samples

The chemical compositions of mussel and cockle shells before and after calcination at 900°C for 5 hours are summarized in Table 1. The XRF results confirm that calcium oxide (CaO) is the dominant component in all samples, exceeding 99% both before and after heat treatment. This highlights the naturally high calcium carbonate ($CaCO_3$) content in mollusk shells, making them suitable precursors for CaO production. After calcination, a slight increase in CaO content was observed in both shell types: from 99.011% to 99.139% in mussel shells and from 99.041% to 99.287% in cockle shells. This increase is attributed to the thermal decomposition of $CaCO_3$ into CaO with the release of CO_2 gas. As CO_2 is removed during heating, the relative proportion of CaO increases, indicating successful conversion into the oxide phase, as follows:

$$CaCO_3\,(s) \xrightarrow{900°C} CaO\,(s) + CO_2\,(g) \qquad (3)$$

In addition to CaO, trace amounts of other oxides including Fe_2O_3, MgO, and SrO were detected. Fe_2O_3 was found at levels below 0.03% in all samples. Mussel shells showed a slight decrease in Fe_2O_3 upon calcination (0.010% → 0.005%), while cockle shells exhibited a small increase (0.012% → 0.023%). These variations may result from mineral transformations or redistribution of minor constituents during high-temperature treatment. MgO and SrO were also present in low concentrations (0.25 – 0.62%). Both oxides decreased after calcination in each shell type, suggesting either volatilization of trace minerals or decomposition of associated compounds at elevated temperature. These findings are consistent with those reported by Boonyuen et al., and Kamba et al. (Boonyuen et al., 2015; Kamba et al., 2013), who found that shell materials in Thailand typically contain more than 99% CaO, making them suitable raw materials for use in adsorbents, catalysts, or ceramic production. Despite these minor changes, their overall content remained very low and did not significantly influence the purity of the resulting CaO. Overall, the XRF analysis confirms that both mussel and cockle shells contain exceptionally high CaO content after calcination, with minimal impurities. This supports their suitability as alternative bio-derived CaO sources for use in glass fabrication, ceramics, catalysts, and environmental applications. The purity levels observed align well with previous reports on calcium-rich shell materials, reaffirming their potential as sustainable and cost-effective raw materials.

Table 1. XRF data of mussel and cockle shells.

Oxide Component	Mussel shell		Cockle shells	
	Before heating	After heating	Before heating	After heating
CaO (%)	99.011	99.139	99.041	99.287
Fe_2O_3 (%)	0.010	0.005	0.012	0.023
MgO (%)	0.469	0.437	0.621	0.437
SrO (%)	0.511	0.419	0.325	0.253

The crystal structure characteristics of cockle shells, before and after calcination at 900°C for 5 hours, were investigated using X-ray diffraction (XRD) analysis to identify the crystalline phases present in the samples. As shown in Figure 3, the diffraction patterns of both mussel and cockle shells prior to calcination exhibited characteristic peaks corresponding to calcium carbonate ($CaCO_3$) in the orthorhombic aragonite phase, as referenced by the crystallographic database COD no. 9016223. Prominent peaks were observed at diffraction angles (2θ) of approximately 26°, 33°, 38°, and 47°, confirming that $CaCO_3$ is the primary crystalline phase in the natural shell samples. After calcination at 900°C, significant changes in the crystal structure were observed. The characteristic peaks of $CaCO_3$ diminished or disappeared entirely, while new peaks appeared corresponding to calcium oxide (CaO) with a cubic crystal structure (space group Fm-3m), in accordance with COD no. 9006712. The most intense peaks for CaO were found at approximately 2θ = 37°, 54°, and 64°. This transformation is attributed to the thermal decomposition of calcium carbonate according to the following reaction (3). The decomposition disrupts the original $CaCO_3$ crystal lattice, resulting in the formation of a new CaO phase with a distinctly different crystal structure. These findings are consistent with previous studies such as Boonyuen et al.

(2015), which reported that heating shells or limestone above 800°C induces the decomposition of $CaCO_3$ into CaO, a product widely used in industrial applications including cement and ceramics manufacturing. Furthermore, the disappearance of $CaCO_3$ peaks and the emergence of CaO peaks after calcination serve as reliable indicators of the completeness of the calcination process, confirming the effective conversion of natural shell materials into high-purity oxide compounds.

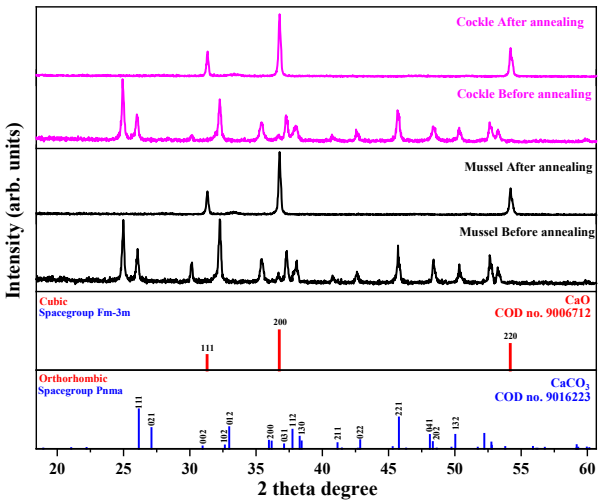

Figure 3. X-ray diffraction (XRD) patterns of mussel and cockle shells before and after calcination at 900°C for 5 hours.

3.2 Analysis of density, molar volume, and refractive index

Glass samples were prepared using calcium oxide (CaO) from different sources: commercial CaO, CaO synthesized from mussel shells, and CaO derived from cockle shells. All glass samples were transparent, clear, and colorless, indicating high-quality melting and forming processes without impurities or bubbles in the glass matrix (as shown in Figure 4). The measured densities of the glass samples are summarized in Table 2. The glass prepared from commercial CaO exhibited a density of 2.7604 ± 0.002 g/cm³, while the glasses derived from mussel shell CaO and cockle shell CaO showed similar densities of 2.7593 ± 0.001 and 2.7626 ± 0.001 g/cm³, respectively. These results suggest that the structural composition and purity of CaO extracted from biological sources (shells) have minimal impact on the density of the glass matrix. Moreover, the slight differences observed in density values were not statistically significant. Regarding the molar volume, the commercial CaO-based glass had a molar volume of 43.0495 ± 0.025 cm³/mol, whereas the mussel shell and cockle shell CaO glasses exhibited molar volumes of 43.0665 ± 0.012 and 43.0153 ± 0.023 cm³/mol, respectively. These close values indicate that the atomic-scale structural spacing within the glass matrix is not significantly influenced by the CaO raw material source. For the refractive index, a critical optical property reflecting electron density in the glass structure, the commercial CaO glass showed a value of 1.5351 ± 0.004. Glasses prepared from mussel shell and cockle shell CaO displayed slightly higher refractive indices of 1.5364 ± 0.001 and 1.5365 ± 0.000, respectively. The marginally higher values for shell-derived glasses may be attributed to minor impurities in the natural raw materials, which could slightly affect light scattering within the glass matrix.

In summary, all results indicate that CaO obtained from mussel and cockle shells can effectively replace commercial CaO in glass production without adversely affecting the physical or optical properties of the resulting glass. This finding supports the sustainable use of renewable biological materials in advanced material manufacturing.

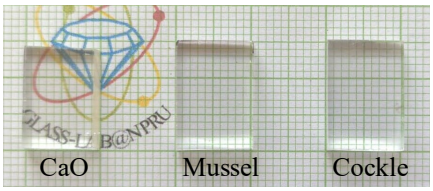

Figure 4. Glass samples prepared using commercial CaO, mussel shell-derived CaO, and cockle shell-derived CaO.

Table 2. Density, molar volume, and refractive index of glass samples.

Glass Sample	Density (g/cm³)	Molar Volume (cm³/mol)	Refractive Index
Commercial CaO	2.7604 ± 0.002	43.0495 ± 0.025	1.5351 ± 0.004
Mussel Shell CaO	2.7593 ± 0.001	43.0665 ± 0.012	1.5364 ± 0.001
Cockle Shell CaO	2.7626 ± 0.001	43.0153 ± 0.023	1.5365 ± 0.000

3.3 Absorption spectra analysis

The absorption spectra analysis revealed that all three glass samples exhibited similar spectral features, with absorption peaks occurring at nearly identical wavelengths. These peaks correspond to the characteristic absorption bands of Sm^{3+} ions, attributed to electronic transitions from the ground state ($^6H_{5/2}$) to various higher excited states (Carnall et al., 1968), as shown in Figure 5. The absorption spectra of the three samples exhibit similar peak positions corresponding to the characteristic f–f transitions of Sm^{3+}, although slight variations in absorption intensity are observed. This suggests that CaO derived from mussel and cockle shells can effectively replace commercial CaO without compromising the doping efficiency of the luminescent ions. Moreover, the well-defined f–f transition peaks, which are characteristic of Sm^{3+}, further confirm a good dispersion of Sm^{3+} ions within the glass network. There is no evidence of phase separation or crystallization that would otherwise distort or blur the absorption bands. These results support the suitability of bio-derived CaO in the fabrication of optical glass materials for photonic applications.

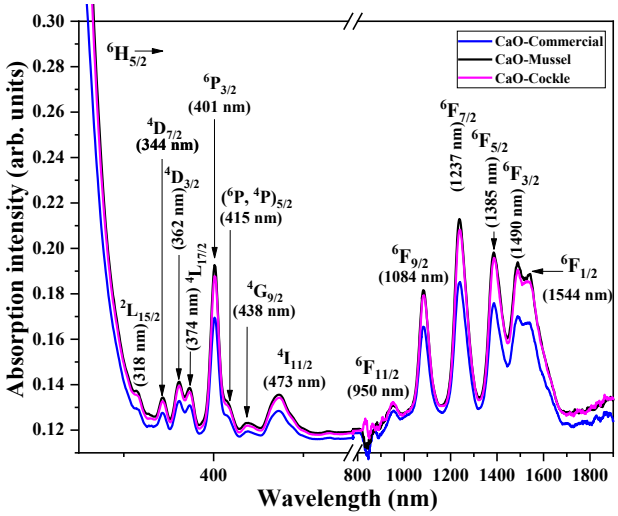

Figure 5. Absorption spectra of the glass samples prepared using commercial CaO, CaO from mussel shells, and CaO from cockle shells.

3.4 Photoluminescence spectra analysis

The excitation spectra presented in Figure 6 (a), measured in the wavelength range of approximately 200–500 nm using a Cary Eclipse Fluorescence Spectrophotometer, correspond to glass samples doped with Sm^{3+} prepared using CaO from different sources. The spectra exhibit distinct excitation peaks that can be attributed to the intra-4f transitions of Sm^{3+}, particularly from the ground state $^6H_{5/2}$ to various excited states responsible for

luminescence. The intensive excitation band at around 204 nm is due to the absorption of Sm^{3+}–O^{2-} charge transfer band (CTB). The most prominent peak appears at 401 nm, which corresponds to the most efficient excitation transition, commonly used to induce emission from Sm^{3+} around 597 nm. The excitation spectra of all three glass samples, those prepared from commercial CaO, mussel shell-derived CaO, and cockle shell-derived, show nearly identical peak positions, while small variations in band intensity occur, which may be attributed to differences in the local structural surroundings of Sm^{3+}, particularly at the dominant peak at 401 nm. This similarity indicates that the local environment of Sm^{3+} within the glass matrix is not significantly affected by the source of CaO, suggesting that bio-derived CaO can effectively replace commercial CaO without negatively impacting the excitation behavior of Sm^{3+} ions. The emission behavior of the Sm^{3+} doped phosphate glasses was investigated in the wavelength range of 500–750 nm, following excitation at 401 nm.

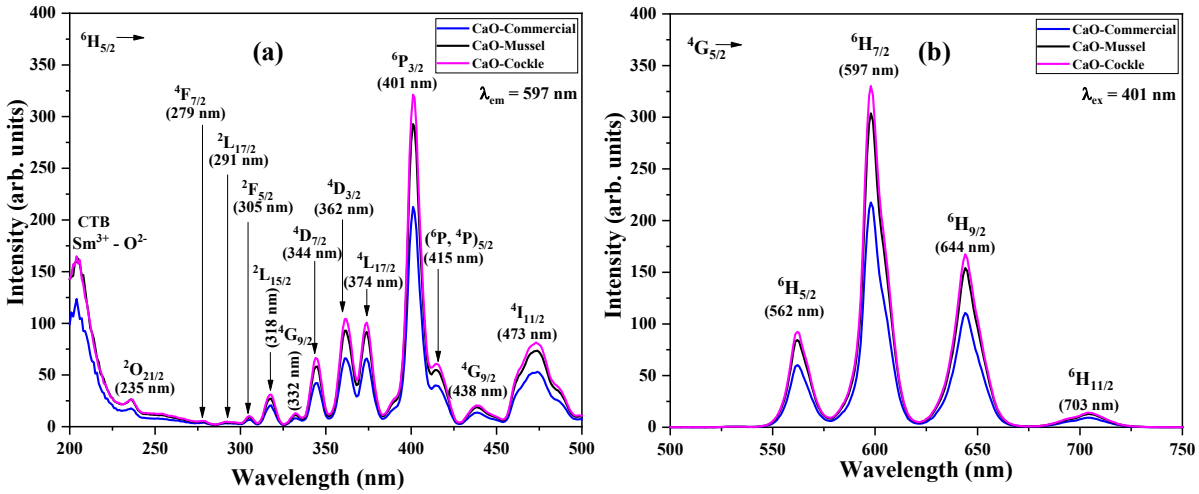

Figure 6. (a) Excitation spectra and (b) emission spectra of the glass samples prepared using commercial CaO, CaO derived from mussel shells, and CaO derived from cockle shells.

Upon excitation, Sm^{3+} ions are promoted to higher energy states and undergo non-radiative relaxation down to the metastable $^4G_{5/2}$ level, primarily through phonon interactions within the glass matrix. Subsequently, radiative transitions occur to lower energy levels, resulting in the emission of characteristic peaks. As shown in Figure 6 (b), four distinct emission peaks are observed at 562, 597, 644, and 703 nm. These correspond to the transitions from the excited $^4G_{5/2}$ state to the lower energy states $^6H_{5/2}$, $^6H_{7/2}$, $^6H_{9/2}$, and $^6H_{11/2}$, respectively (Carnall et al., 1968). Among these, the transition at 597 nm ($^4G_{5/2}\rightarrow{}^6H_{7/2}$) is the most intense, producing orange-red emission. When comparing the emission intensities, glass samples prepared from mussel and cockle shells exhibited slightly higher emission intensities than those made with commercial CaO, with the cockle-derived sample showing the highest intensity among the three. This enhancement may be attributed to subtle differences in the glass structure and the local symmetry around the Sm^{3+} ions introduced by the varying sources of CaO. The higher intensity observed in the bio-derived CaO samples indicates a comparable or potentially superior capability for light absorption and emission relative to the commercial CaO-derived glass, further supporting the viability of using renewable biogenic CaO as a sustainable alternative in photonic glass applications.

3.5 Luminescence color analysis in the CIE 1931 color coordinate system

The luminescence color of the glass samples was analyzed based on the standards of the Commission Internationale de l'Eclairage (CIE). The measured color coordinates (X, Y) for each sample are shown in Table 3, and the corresponding chromaticity points were plotted on the CIE 1931 chromaticity diagram, as illustrated in Figure 7. The results indicate that all glass samples exhibit closely similar chromaticity coordinates,

suggesting minimal variation in their emitted color. The coordinates fall within the orange-red region of the visible spectrum, confirming that the glasses emit light in this color range when excited at a wavelength of 401 nm. These findings validate the consistency of luminescent color among the three glass types, regardless of whether CaO was derived from commercial sources, mussel shells, or cockle shells. Therefore, biogenic CaO sources are suitable alternatives for fabricating luminescent phosphate glasses without compromising chromatic performance.

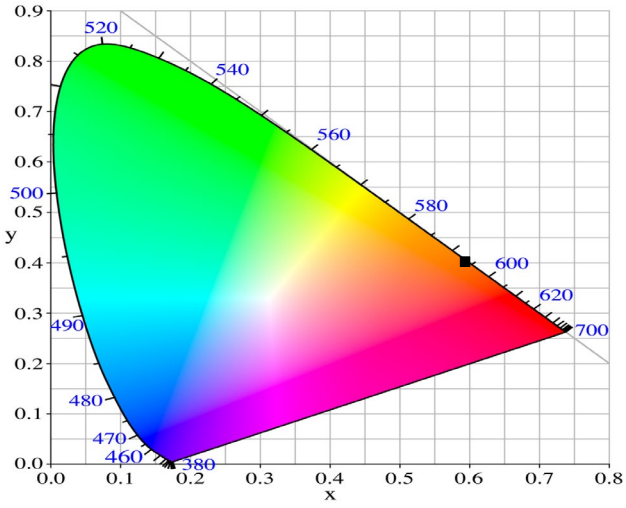

Figure 7. CIE 1931 chromaticity diagram showing the luminescence color coordinates of glass samples prepared using commercial CaO, mussel shell-derived CaO, and cockle shell-derived CaO.

Table 3. CIE color coordinates (x, y) of the glass samples.

Glass Sample	CIE Coordinate (x, y)
Commercial CaO	(0.5937, 0.4055)
Mussel Shell CaO	(0.5936, 0.4057)
Cockle Shell CaO	(0.5935, 0.4057)

3.6 Luminescence lifetime analysis

The luminescence lifetime refers to the time during which the Sm^{3+} ions remain in an excited state before returning to the ground state and releasing energy in the form of light. This parameter is typically expressed in milliseconds (ms). In this study, the lifetime measurements were conducted under excitation at 401 nm, with emission monitored at 597 nm, which corresponds to the main emission transition of Sm^{3+}. The results indicate that the glass sample prepared using commercial CaO exhibited the shortest lifetime of 1.260 ms. In contrast, the samples made using biogenic CaO sources (mussel and cockle shells) showed slightly longer lifetimes, with the mussel shell-derived CaO yielding the highest value of 1.358 ms, as illustrated in Figure 8.

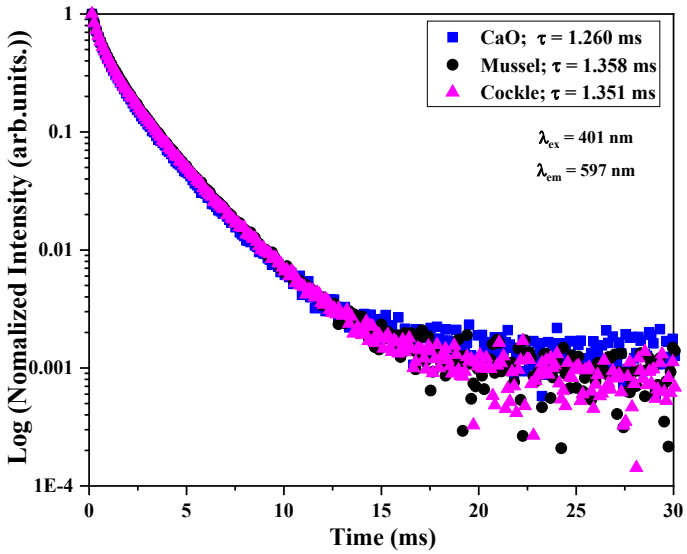

Figure 8. Luminescence decay curves showing the lifetime of the emission transition from the excited state to the $^4G_{5/2}$ energy level of Sm^{3+} ions in glass samples prepared from commercial CaO, mussel shell-derived CaO, and cockle shell-derived CaO.

The observed increase in luminescence lifetime for the bio-derived CaO samples suggests that Sm^{3+} ions reside in a local environment with reduced non-radiative relaxation pathways likely due to lower phonon energy and fewer quenching centers in the glass network. Such enhanced lifetimes are advantageous for luminescent materials used in optoelectronic devices, phosphors for LEDs, and optical sensors, where prolonged and stable emission is desired.

3.7 Judd – Ofelt (J-O)analysis and radiative properties

The most widely used technique for spectroscopic investigation of Ln^{3+} ions in different environments is the Judd–Ofelt (J-O) theory. The experimental oscillator strengths (f_{exp}) are determined from the absorption spectra by integrating the areas under the absorption peaks. In contrast, the theoretical oscillator strengths (f_{cal}) are calculated using the J-O theory, as described in previous studies (Ichoja et al., 2020; Rayappan & Marimuthu, 2013).

Table 4. Wavelength (nm), experimental (f_{exp}) and calculated (f_{cal}) oscillator strengths ($\times 10^{-6}$, cm^2) along with J–O intensity parameters Ω_λ ($\times 10^{-20}$ cm^2) and δ_{rms} deviations for glass samples prepared from commercial CaO, mussel shell-derived CaO, and cockle shell-derived CaO.

Transitions $^6H_{5/2} \rightarrow$	λ (nm)	CaO-commercial		CaO-mussel		CaO-cockle	
		f_{exp}	f_{cal}	f_{exp}	f_{cal}	f_{exp}	f_{cal}
$^4D_{7/2}$	344	0.18	0.01	0.27	0.01	0.27	0.02
$^4D_{3/2}$	362	0.38	0.38	0.52	0.45	0.46	0.40
$^4L_{17/2}$	374	0.35	0.00	0.40	0.00	0.36	0.00
$^6P_{3/2}$	401	1.32	2.30	1.87	2.74	1.69	2.42
$^4G_{9/2}$	438	0.05	0.05	0.03	0.05	0.01	0.06
$^4I_{11/2}$	473	0.24	0.12	0.35	0.14	0.24	0.16
$^6F_{11/2}$	950	0.13	0.29	0.16	0.33	0.17	0.37
$^6F_{9/2}$	1084	0.55	1.77	0.76	1.99	0.86	2.25
$^6F_{7/2}$	1237	3.33	2.47	3.68	2.82	4.02	3.03
$^6F_{5/2}$	1385	1.18	1.14	1.35	1.38	1.19	1.22
$^6F_{3/2}$	1490	0.22	0.58	0.46	0.75	0.29	0.68
$^6F_{1/2}$	1544	0.35	0.10	0.40	0.20	0.49	0.20
δ_{rms}		0.547		0.536		0.572	
Ω_2		0.32		0.62		0.65	
Ω_4		2.21		2.63		2.32	
Ω_6		2.13		2.38		2.74	

Table 4 shows that for absorption peaks, the discrepancies between f_{cal} and f_{exp} are fairly small, indicating good agreement between the experimental results and theoretical predictions. Furthermore, the highest f values are observed for the $^6H_{5/2} \rightarrow {}^6F_{7/2}$ (1237 nm) transition, which is known to be hypersensitive and strongly influenced by the ligand environment surrounding the Sm^{3+} ions. This transition is classified as hypersensitive because it satisfies the selection rules $|\Delta S| = 0$, $|\Delta L| \leq 2$, and $|\Delta J| \leq 2$, and its intensity is highly affected by the chemical environment around the rare-earth ion sites. The J-O intensity parameters (Ω_λ, $\lambda = 2$, 4 and 6) were also derived using the J-O theory and are presented in the same table. In general, the Ω_2 parameter provides information about the asymmetry of the coordination structure and the covalent nature of the Ln–O bond. A higher Ω_2 value indicates a more asymmetric environment. In contrast, the Ω_4 and Ω_6 parameters are related to the basicity, rigidity, and viscosity of the glass matrix (Lachheb et al., 2018).

Among all prepared glasses, the CaO-cockle glass exhibits the highest Ω_2 value (0.65×10^{-6} cm^2), compared to CaO-commercial (0.62×10^{-6} cm^2) glass and CaO-mussel (0.32×10^{-6} cm^2) glass indicating the strongest Sm–O covalency and the most asymmetric Sm^{3+} environment. The greater asymmetry in the CaO-cockle glass leads to higher emission intensity compared to CaO-commercial and CaO-mussel glass, as previously discussed. In addition, the higher Ω_4 and Ω_6 values for CaO-cockle glass suggest greater viscosity and rigidity in its glass matrix.

Radiative properties such as radiative transition probabilities (A_R), stimulated emission cross-sections (σ_e), and branching ratios (β) for the excited states of Sm^{3+} ions were estimated using the J–O parameters and the refractive index, based on equations reported in the literature (Reddy et al., 2017). The results are presented in Table 5. However, some parameters show the highest values in the CaO-cockle glass. In particular, the CaO-cockle sample provides the highest stimulated emission cross-section ($\sigma_e = 4.929\times10^{-22}$ cm^2) for the $^4G_{5/2} \rightarrow {}^6H_{7/2}$ transition, slightly higher than those of the CaO-mussel (4.888×10^{-22} cm^2) and CaO-commercial glasses (4.338×10^{-22} cm^2). According to the A_R values, the most probable radiative transition in all samples is the $^4G_{5/2} \rightarrow {}^6H_{7/2}$ emission at 597 nm. The β value also confirms this, as all prepared glasses exhibit the highest β for this transition. These radiative parameters collectively indicate the strong orange-red emission behavior characteristic of Sm^{3+} activated glasses.

Table 5 Transition probabilities (A_R, s^{-1}), branching ratios experiment (β_{exp}) and calculated (β_{rad}), radiative lifetimes (τ_R, ms), stimulated emission cross-sections (σ_e, $\times10^{-22}$ cm^2) and quantum efficiency (η, %) for the observed emission transitions of glass samples prepared from commercial CaO, mussel shell-derived CaO, and cockle shell-derived CaO.

Glasses	Transitions	A_R	β_{exp}	β_{rad}	σ_e	τ_R	η
CaO-commercial	$^4G_{5/2} \rightarrow {}^6H_{5/2}$	17.12	0.1346	0.1039	0.781	6.61	19.07
	$^4G_{5/2} \rightarrow {}^6H_{7/2}$	79.95	0.5242	0.4852	4.338		
	$^4G_{5/2} \rightarrow {}^6H_{9/2}$	32.41	0.3131	0.1967	2.023		
	$^4G_{5/2} \rightarrow {}^6H_{11/2}$	17.39	0.0281	0.1056	1.340		
CaO-mussel	$^4G_{5/2} \rightarrow {}^6H_{5/2}$	17.88	0.1385	0.0932	0.792	5.21	26.05
	$^4G_{5/2} \rightarrow {}^6H_{7/2}$	90.81	0.5209	0.4735	4.888		
	$^4G_{5/2} \rightarrow {}^6H_{9/2}$	42.16	0.3108	0.2198	2.609		
	$^4G_{5/2} \rightarrow {}^6H_{11/2}$	20.43	0.0299	0.1056	1.525		
CaO-cockle	$^4G_{5/2} \rightarrow {}^6H_{5/2}$	17.50	0.1362	0.0921	0.788	5.26	25.67
	$^4G_{5/2} \rightarrow {}^6H_{7/2}$	91.70	0.5197	0.4826	4.929		
	$^4G_{5/2} \rightarrow {}^6H_{9/2}$	40.63	0.3118	0.2138	2.497		
	$^4G_{5/2} \rightarrow {}^6H_{11/2}$	19.47	0.0322	0.1024	1.386		

Radiative lifetimes (τ_R) were obtained from the sum of the radiative transition probabilities (A_R) for the observed transitions. Using the experimentally measured luminescence lifetimes (τ_{exp}) under excitation at 401 nm and emission monitored at 597 nm, the internal quantum efficiency η was calculated as $\eta = (\tau_{exp} / \tau_R) \times 100\%$. The calculated quantum efficiencies are 19.07% (commercial CaO), 26.05% (mussel shell CaO), and 25.67% (cockle shell CaO). The higher quantum efficiencies of the bio-derived CaO glasses are primarily due to their longer experimentally measured lifetimes combined with comparable or slightly shorter radiative lifetimes, indicating reduced non-radiative decay rates in these samples. These results are consistent with the observation of

slightly enhanced emission intensities in the shell-derived CaO samples. Nevertheless, the overall moderate values of η (≈20–26%) indicate that non-radiative pathways remain significant in this glass host and that further optimization (for example, reducing high-energy phonons or structural defects) would be required to improve quantum efficiency for device applications.

Based on the results presented above including emission spectra, Judd–Ofelt (J-O) parameters, and radiative properties, it can be concluded that a high degree of asymmetry in the glass structure significantly influences its fluorescence properties. Among the studied samples, CaO-cockle glass exhibits superior performance compared to CaO-commercial glass and CaO-mussel glass, suggesting its strong potential as an optimal host material for possible applications in the manufacturing of display and optoelectronic devices in the orange region.

4. Conclusions

This study investigated the use of calcium oxide (CaO) extracted from mussel and cockle shells as a precursor for preparing Sm^{3+} doped glass, comparing the results with glass prepared from commercial CaO. The key findings are as follows:

- Chemical composition analysis by XRF revealed that CaO derived from shell sources has purity comparable to commercial CaO, with CaO content exceeding 99.97% in all cases.
- XRD analysis showed that CaO obtained by calcining the shells forms a complete CaO phase without detectable impurities.
- Physical properties including density, molar volume, and refractive index of glasses prepared from shell-derived CaO were close to those of glasses prepared from commercial CaO, with no statistically significant differences.
- Optical properties investigated through UV-Vis-NIR absorption, excitation, and emission spectra demonstrated that the shell-derived CaO glasses exhibited absorption and emission peaks similar to those of commercial CaO glasses. Notably, the emission intensity was slightly higher, indicating a suitable host structure for efficient absorption and emission of Sm^{3+} ions.
- Luminescence lifetime measurements showed that glasses made from mussel shell CaO had the longest lifetime (1.358 ms), followed by cockle shell CaO (1.351 ms), and commercial CaO (1.260 ms), indicating reduced non-radiative losses and improved luminescence efficiency.
- CIE 1931 chromaticity coordinates indicated that all samples emitted orange-red light, making them promising for applications in display technologies and LED light sources.
- The Judd–Ofelt (J–O) analysis, the highest oscillator strengths were observed for the hypersensitive transitions, which are strongly influenced by the ligand environment around Sm^{3+} ions.
- Among the J–O intensity parameters, the Ω_2 parameter clearly revealed variations in local asymmetry and covalency of the Sm–O bonds. Notably, the CaO-cockle glass showed the highest Ω_2 value, suggesting the most asymmetric local environment, which in turn enhances electric dipole transitions and emission intensity.
- Radiative properties, including transition probabilities, branching ratios, and stimulated emission cross-sections, were also estimated and support these findings.
- Overall, the CaO-cockle glass demonstrates superior fluorescence performance compared to the CaO-commercial and CaO-mussel glasses, highlighting its strong potential as an efficient host material for orange-emitting optoelectronic and display applications.

Overall, CaO extracted from mussel and cockle shells demonstrates high potential as a sustainable alternative to commercial CaO for producing Sm^{3+} doped glass, without compromising structural, physical, optical, or color properties. This approach promotes the utilization of renewable resources, reduces natural waste, and adds economic value in an environmentally friendly manner.

Acknowledgements

The authors would like to thank National Research Council of Thailand (NRCT), Thailand Science Research and Innovation (TSRI), Center of Excellence in Glass Technology and Materials Science (CEGM) and Nakhon Pathom Rajabhat University for supporting this research.

References

Ataullah, Khan, I., Khattak, S., Shoaib, M., Kaewkhao, J., Ullah, I., & Rooh, G. (2021). Spectral investigation of lithium-telluride based glasses doped with Sm^{3+}-ions for lighting application. *Journal of Alloys and Compounds*, *875*, 160095. https://doi.org/10.1016/j.jallcom.2021.160095

Bamigboye, G. O., Nworgu, A. T., Odetoyan, A. O., Kareem, M., Enabulele, D. O., & Bassey, D. E. (2021). Sustainable use of seashells as binder in concrete production: Prospect and challenges. *Journal of Building Engineering*, *34*, 101864. https://doi.org/10.1016/j.jobe.2020.101864

Beall, G. H. (1992). Design and properties of glass-ceramics. *Annual Review of Materials Science*, *22*, 91–119. http://dx.doi.org/10.1146/annurev.ms.22.080192.000515

Boonyuen, S., Malaithong, M., Prokaew, A., Cherdhirunkorn, B., & Chuasantia, I. (2015). Decomposition study of calcium carbonate in shells. *Thai Journal of Science and Technology*, *4*(2), 115–122. https://doi.org/10.14456/tjst.2015.10

Carnall, W. T., Fields, P. R., & Rajnak, K. (1968). Electronic energy levels in the trivalent lanthanide aquo ions. I. Pr^{3+}, Nd^{3+}, Pm^{3+}, Sm^{3+}, Dy^{3+}, Ho^{3+}, Er^{3+}, and Tm^{3+}. *The Journal of Chemical Physics*, *49*, 4424–4442. http://dx.doi.org/10.1063/1.1669893

Elkhoshkhany, N., Marzouk, S., El–Sherbiny, M., Atef, M., Damak, K., Alqahtani, M. S., Algarni, H., Reben, M., & Yousef, E. S. (2021). Spectroscopic properties in simple cost glasses with alkaline oxides doped with Sm_2O_3 for display laser emission. *Results in Physics*, *31*, 104955. https://doi.org/10.1016/j.rinp.2021.104955

Ellen MacArthur Foundation. (2013). *Towards the circular economy: Economic and business rationale for an accelerated transition*.

Ichoja, A., Hashim, S., Ghoshal, S. K., & Hashim, I. H. (2020). Absorption and luminescence spectral analysis of Dy^{3+}-doped magnesium borate glass. *Chinese Journal of Physics*, *66*, 307–317. https://doi.org/10.1016/j.cjph.2020.03.029

Isac, S. J., Vinothkumar, P., Dhinakaran, A. P., & Praveenkumar, S. (2025). Physical, optical, and luminescent characteristics of Sm^{3+} doped tellurite glass suitable for yellow laser, warm white LED, and radiation shielding applications. *Optics and Laser Technology*, *182*, 112111. https://doi.org/10.1016/j.optlastec.2024.112111

Kamba, A. S., Ismail, M., Ibrahim, T. A. T., & Zakaria, Z. A. B. (2013). Synthesis and characterisation of calcium carbonate aragonite nanocrystals from cockle shell powder (*Anadara granosa*). *Journal of Nanomaterials*, *2013*, 398357. https://doi.org/10.1155/2013/398357

Kumar, V. R., Nagaraju, G., Asirvadam, A., Reddy, A. S. S., & Ashok, J. (2019). Spectroscopic properties of Nd^{3+} doped $PbO\text{-}Sb_2O_3\text{-}CaO/MgO/SrO$ glasses. *Materials Today: Proceedings*, *19*, 2663–2667. https://doi.org/10.1016/j.matpr.2019.10.120

Lachheb, R., Herrmann, A., Assadi, A. A., Reiter, J., Körner, J., Hein, J., Rüssel, C., Maâlej, R., & Damak, K. (2018). Judd–Ofelt analysis and experimental spectroscopic study of erbium doped phosphate glasses. *Journal of Luminescence*, *201*, 245–254. https://doi.org/10.1016/j.jlumin.2018.03.087

Mignardi, S., Tocci, E., & Medeghini, L. (2024). Clam shell waste recycling and valorization for sustainable Hg remediation. *Heliyon*, *10*, e35375. https://doi.org/10.1016/j.heliyon.2024.e35375

Rayappan, I. A., & Marimuthu, K. (2013). Structural and luminescence behavior of the Er^{3+} doped alkali fluoroborate glasses. *Journal of Non-Crystalline Solids*, *367*, 43–50. https://doi.org/10.1016/j.jnoncrysol.2013.02.016

Reddy, B. N. K., Raju, B. D., Thyagarajan, K., Ramanaiah, R., Jho, Y.-D., & Reddy, B. S. (2017). Optical characterization of Eu^{3+} ion doped alkali oxide modified borosilicate glasses for red laser and display device applications. *Ceramics International*, *43*, 8886–8892. https://doi.org/10.1016/j.ceramint.2017.04.024

Selvi, S., Marimuthu, K., & Muralidharan, G. (2015). Structural and luminescence behavior of Sm^{3+} ions doped lead boro-telluro-phosphate glasses. *Journal of Luminescence*, *159*, 207–218. http://dx.doi.org/10.1016/j.jlumin.2014.11.025